Kinetics of selective oxidation of dimethyl ether to formaldehyde over Al_2O_3-supported VO_x and MoO_x catalysts

Xiumin Huang, Yonggang Li, Yide Xu, and Wenjie Shen*

State Key Laboratory of Catalysis, Dalian Institute of Chemical Physics, Chinese Academy of Sciences, 457 Zhongshan Road, Dalian, 116023, China

Recieved 23 April 2004; accepted 7 July 2004

The kinetic behaviors of dimethyl ether(DME) selective oxidation to formaldehyde were investigated over Al_2O_3-supported VO_x and MoO_x catalysts. It was showed that the reaction is pseudo-zero order with respect to both dimethyl ether and oxygen molecule, suggesting that the reaction of surface intermediate CH_3O* is likely to be the rate-determining step. The apparent activation energies for the target reaction were determined to be 122 kJ/mol over the VO_x/Al_2O_3 catalyst and 125 kJ/mol over the MoO_x/Al_2O_3 catalyst, respectively. With the decrease of contact time, the dimethyl ether conversion decreased linearly, while the selectivity of HCHO increased, indicating that formaldehyde is the preliminary product of the selective oxidation of dimethyl ether.

KEY WORDS: dimethyl ether; selective oxidation; formaldehyde; kinetics; supported VO_x and MoO_x catalysts.

1. Introduction

Compared with methanol synthesis from synthesis gas, the similar process of dimethyl ether (DME) production from the same feed provides more economically attractive advantages by breaking the thermodynamic restriction, which lead to higher single-pass CO conversion [1]. These great economical potential and environmental benign features of this process make DME an attractive raw material for replacing methanol to produce formaldehyde, acetic acid, and olefins, etc. [2–3], and consequently, lead to the emergence of DME catalytic reaction chemistry. As a matter of fact, the surface methoxide intermediate (CH_3O) involved in methanol reactions can also be generated by the cleavage of the CH_3OCH_3 molecule over metal oxide catalysts under mild reaction conditions [4].

Particularly, the selective oxidation of DME to formaldehyde (HCHO) has attracted much attention in recent years [3]. MoO_x and VO_x supported on Al_2O_3, ZrO_2 and SnO_2 were reported to be reactive for DME selective oxidation to formaldehyde around 550 K, which is much lower than the required temperature of conventional production of formaldehyde via oxidative dehydrogenation of methanol on iron molybdates or Ag-based catalysts [5–6]. Both the conversion of DME and the selectivity to HCHO increased with the MoO_x or VO_x surface density up to their monolayer dispersion capacities [7–9]. Raman and X-ray absorption spectroscopies were used to probe the structure of the MoO_x domains with the observation that the MoO_x domain surfaces become more active as two-dimensional monolayers formed through oligomerization of monomer MoO_x species. Meanwhile, the redox properties of MoO_xdomains also influence DME reaction [7]. The initial H_2 reduction rate of the MoO_x species related to the C–H bond activation of the CH_3O* intermediate was linearly correlated with the DME reaction rate [9]. Modification of the Al_2O_3 support with reducible oxides, which made the MoO_x domains more reducible, led to higher DME reaction rates, while maintaining the HCHO selectivity nearly constant [10]. It is generally accepted that the two-dimensional monolayer MoO_x is more active for the dehydrogenation of adsorbed methoxide species by lattice oxygen, which is regarded as the rate-determining step of DME oxidation. However, most of the previous studies were focused on MoO_x catalysts, and only few investigations have been conducted on VO_x catalysts. Our recent studies showed that Al_2O_3 supported VO_x catalysts even gave better catalytic activities than that of MoO_x catalysts, e.g., lower reaction temperatures could be applied to obtain the same DME conversion over supported VO_x catalyst [8].

In this work, kinetic studies on the selective oxidation of DME to HCHO over Al_2O_3 supported VO_x and MoO_x catalysts were carried out with the aim to establish the reaction kinetic models and to explore the detailed reaction mechanism.

2. Experimental

2.1. Catalyst preparation

A commercially available γ-Al_2O_3 with a BET surface area of 227 m^2/g was used to load V_2O_5 by the wet-impregnation method, in which the desirable amount of ammonium metavanadate (18% of V_2O_5 by weight

*To whom correspondence should be addressed.
E-mail: shen98@dicp.ac.cn

1011-372X/04/0900–0185/0 © 2004 Plenum Publishing Corporation

with respect to the final catalyst) was dissolved in 0.4 M oxalic acid solution at a molar ratio of $V : H_2C_2O_4 = 2 : 1$. The excess water was then evaporated at 323 K. A 30 wt% MoO_3/Al_2O_3 catalyst, having the same amount of active metal atoms as that of 18 wt% V_2O_5/Al_2O_3, was prepared by the incipient wetness impregnation of the γ-Al_2O_3 with an aqueous ammonium heptamolybdate ($(NH_4)_6Mo_7O_{24} \cdot 4H_2O$) solution. Both samples obtained were dried at 373 K overnight and then calcined at 773 K for 3 h in air. The catalysts were pressed, crushed, and sieved to 40–60 meshes for reaction test.

2.2. Catalysts characterization

2.2.1. Surface area

Surface areas were measured by nitrogen adsorption at 97 K using a Micrometrics ASAP 2010 micropore-size analyzer. The specific surface area was determined using the linear portion of the BET model. Prior to these measurements, the samples were degassed in vacuum at 573 K for 2 h.

2.2.2. X-ray photoelectron spectroscopy

An AMICAS spectrometer (KROTAS instrument, Shimadzu) with an X-ray gun for Mg Kαradiation was used. The XPS spectra were taken at room temperature in high vacuum to study the oxidation state of samples prior to reaction. The spectra were corrected with respect to the C 1s energy at 284.7 eV.

2.3. Kinetic investigation

The selective oxidation of DME was carried out in a fixed-bed quartz flow reactor. 50 mg catalyst sample was diluted with the same volume of acid-washed quartz powder (200 mg) in order to avoid temperature gradients in the catalyst bed. Prior to reaction, the catalyst was pre-oxidized in 10% O_2/He at 573 K for 1 h to clean out any possible impurities on the surface.

Two reactant gases were introduced through two parallel mass flow controllers. One gas mixture was 8.95% DME/4.5% N_2/He and N_2 was used as an internal standard gas for product analysis. Another gas mixture was 10% O_2/He. The reactor effluents were analyzed by an online gas chromatograph equipped with TCD and FID detectors. A TDX-01 and Porapak Q combined packed column was used for the separation of O_2, N_2, CO, CO_2, H_2O, HCHO, CH_3OH and DME. A PLOT Q capillary column connected to the FID detector was used for the separation and detection of CH_4, C_2H_4, CH_3OH, DME, and methyl formate.

Reaction orders with respect to DME and oxygen were obtained by changing the flow rate of one gas mixture, while keeping the flow rate of another gas mixture constant. A balance gas of He was introduced to keep the total flow rate constant for all the runs reported here.

The effect of contact time on DME conversion and HCHO selectivity was studied at a constant ratio of DME/O_2. The data was taken at 543 K for the VO_x/Al_2O_3 catalyst, while it was taken at 553 K for the MoO_x/Al_2O_3 catalyst due to its lower activity.

For the determination of the apparent activation energy and the pre-exponential factor, three runs were carried out by changing the molar ratio of DME to oxygen at different temperatures ranging from 513 to 573 K with a total flow rate of 40 ml/min.

3. Results and discussion

3.1. Structural and surface properties

The BET surface areas of supported $30MoO_3/Al_2O_3$ and $18V_2O_5/Al_2O_3$ were 162.1 and 184.2 m^2/g, respectively. XRD measurements showed that the MoO_x is above the monolayer dispersion capacity of Al_2O_3 and VO_x catalyst is slightly lower than the monolayer capacity.

XPS results for both catalysts prior to reaction are listed in figures 1 and 2. It can be seen that the Mo doublet exhibits binding energies at 235.8 eV for Mo $3d_{3/2}$ and 232.7 eV for Mo $3d_{5/2}$, while V doublet exhibits binding energies at 517.6 eV for V $2p_{3/2}$ and at 523.0 eV of V $2p_{1/2}$. Thus, the presence of Mo^{6+} species on the surface of Al_2O_3 can be inferred [11,12]. By considering that standard binding energies of V $2p_{3/2}$ for V^{5+}, V^{4+} and V^{3+} are located at 517.2, 515.9 and 515.3 eV, respectively [13,14], the dominant presence of V^{5+} on the surface of Al_2O_3 can be concluded.

3.2. Assessment of mass-transfer effect

For kinetic studies, the diffusions of the film (external) and the pores (internal) of the catalyst must be eliminated in order to obtain the intrinsic reaction rate. For the submillimeter particle size, the internal mass-transfer retardation usually does not affect gas-phase catalytic reactions. Here, it is considered that the selective oxida-

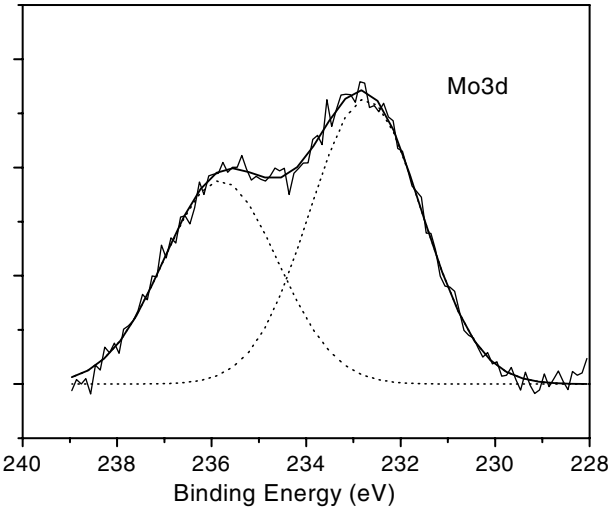

Figure 1. XPS spectra of the Mo 3d in MoO_x/Al_2O_3 catalyst.

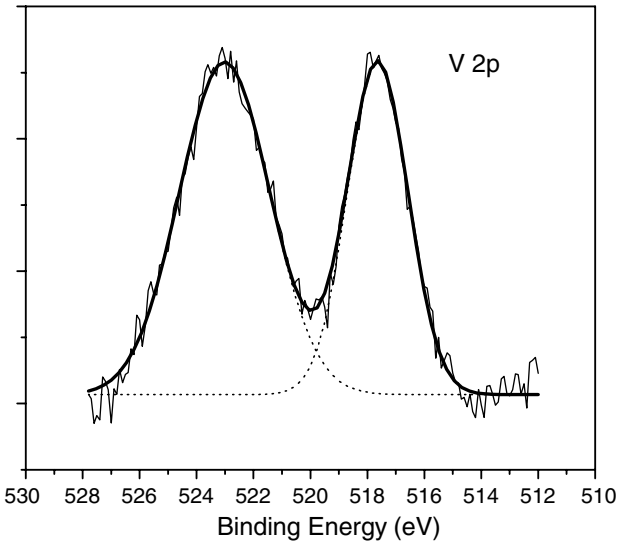

Figure 2. XPS spectra of the V 2p in VO_x/Al_2O_3 catalyst.

tion of DME is an internal diffusion-free reaction because the range of the catalyst particle size employed in the present study is between 250 and 450 μm.

It is well known that oxidation reactions are fast, and thus, the flow rate should be large enough to avoid the existence of any external diffusion. In the present study, two preliminary runs with different amounts of VO_x/Al_2O_3 catalysts were performed at 553 K under a constant ratio of DME/O_2 in the feed. The amount of catalyst in one of the runs was twice larger than that of the other. The feeding rates in these two cases were correspondingly adjusted to yield a constant F/W. It can be seen from table 1 that the conversion of DME was independent of the feeding rate. When the feeding rates were kept constant, the conversion with catalyst loading of 50 mg is about 2.5 times higher as that with 20 mg. These data were obtained in the F/W range of 27–200 ml/g_{cat} min, and the following kinetic investigations was carried out at a F/W range of 44–60 ml/g_{cat} min. Therefore the presence of any external mass-transfer resistance was precluded for the determination of reaction orders, the effects of contact time, and the apparent activation energies.

3.3. Effect of contact time

Figures 3 and 4 show the effect of contact time on the conversion of DME and the selectivity of formaldehyde on the VO_x/Al_2O_3 catalyst and the MoO_x/Al_2O_3 catalyst.

It is clear that the conversion of DME increases linearly with contact time in both cases. The plots of contact time versus conversion of DME are straight lines passing through the origin of the coordinate, indicating that the selective oxidation of DME is a typical heterogonous catalytic surface reaction over the supported VO_x and MoO_x catalysts.

Table 1
Effect of external diffusion on the reaction over VO_x /Al_2O_3 catalyst

Temp. (K)	Cat W (mg)	F(DME/He) (ml/min)	F(O_2/He) (ml/min)	F(He) ml/min	F/W (ml/g_{cat}*min*)	DME (conv.%)
553	25	5	6	14	17.9	13.6
50	10	12	28	17.9	12.6	
543	20	22.5	9	0	100.7	2.02
50	22.5	9	0	40.3	5.21	
20	15	6	0	67.1	3.2	
50	15	6	0	26.8	7.8	

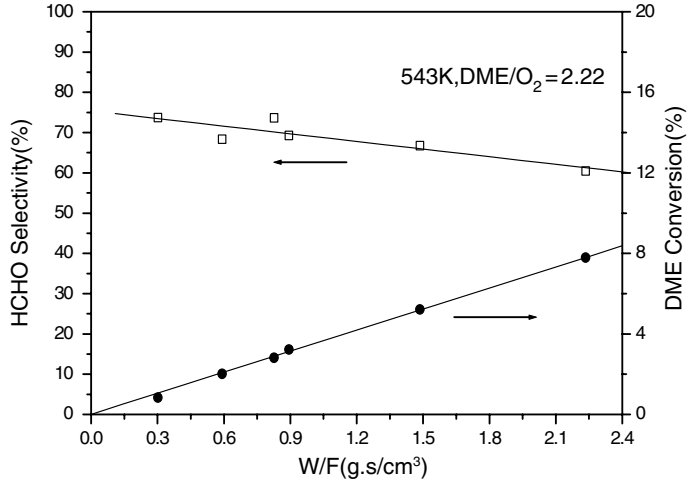

Figure 3. Effect of contact time on the conversion of DME and the selectivity of formaldehyde on VO_x/Al_2O_3 catalyst.

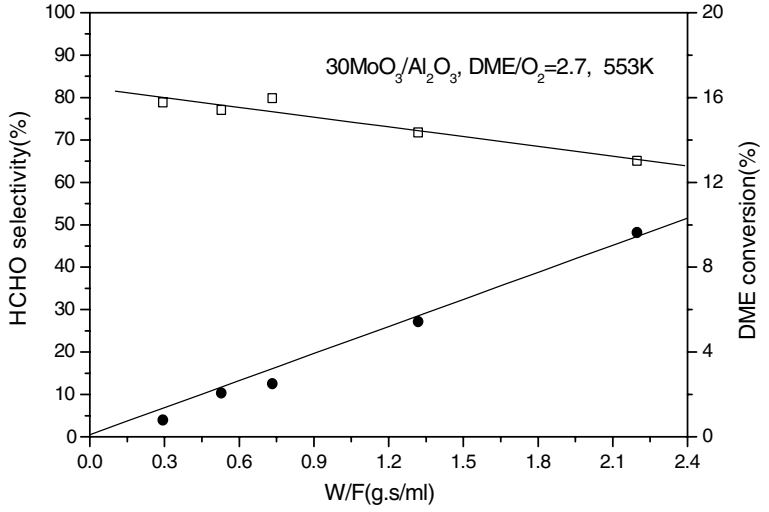

Figure 4. Effect of contact time on the conversion of DME and the selectivity of formaldehyde on MoO_x/Al_2O_3 catalyst.

As can be seen from figures 5 and 6, the selectivity of HCHO decreases with the increasing in the contact time, while the selectivity to CO increases. This kind of formaldehyde selectivitity dependence on the contact time suggests that the primary product in the partial oxidation of DME is HCHO. With the increase in the contact time, the initially formed HCHO would decompose into CO and H_2, or further oxidized to CO_2 and H_2O on the catalyst surface. The primary selectivity of CH_3OH is not equal to zero, implying that it can be produced directly from DME. CH_3OH can be formed by intra-transfer of hydrogen between two CH_3O* species. Moreover, the selectivity to CH_3OH is essentially independent of the contact time, suggesting that the further oxidation of methanol is a relatively slower process.

Meanwhile, the selectivity of CO, which is the main by-product of the reaction, increases with the contact time. This means that CO can be produced by secondary reactions of HCHO. CO can also be formed directly by CH_3* oxidation or by CH_3O* decomposition. The selectivity of CO also increases with the reaction temperature, while the selectivity of CO_2 and methyl formate are very small compared with that of CO.

CH_4 is observed over the Al_2O_3 supported VO_x and MoO_x catalysts only when the oxygen in the feed is depleted. This may suggest that the adsorbed CH_3^* species decomposed from DME is prone to combine with O* to form CH_3O* rather than to combine with the H* that is dehydrogenated from the CH_3O* species over these catalysts. But when the oxygen in the feed is completely depleted at about 593 K on VO_x/Al_2O_3 catalyst, DME would be decomposed into CH_4 via the reaction of $CH_3OCH_3 \rightarrow CH_4 + CO + H_2$ [8]. The decomposition of DME could be observed at 543 K when DME is the only feed-gas over supported VO_x. This means that the existence of oxygen inhibits the

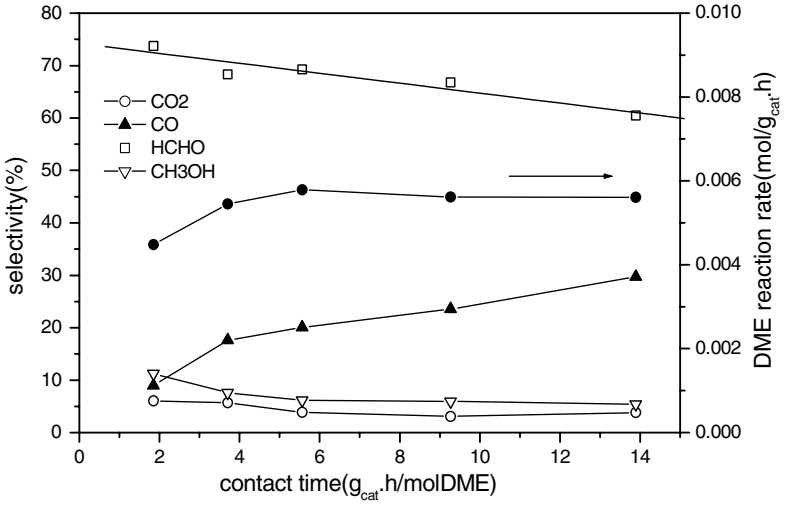

Figure 5. DME reaction rate and product selectivity over VO_x /Al_2O_3 catalyst at 543 K.

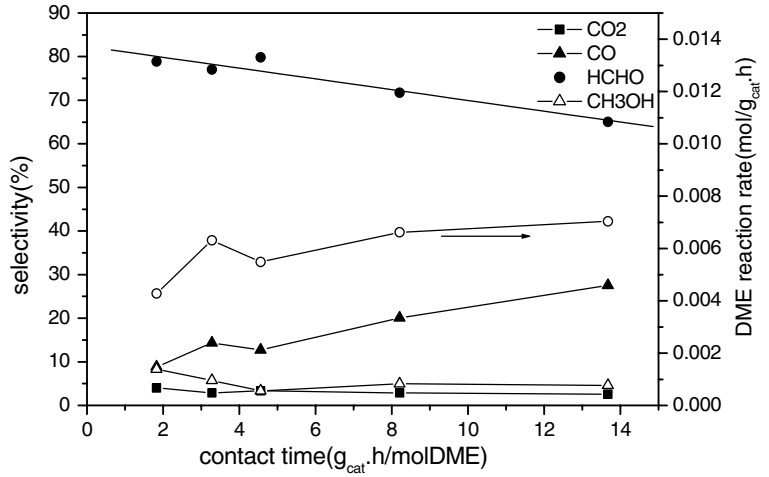

Figure 6. DME reaction rate and product selectivity over MoO_x /Al_2O_3 catalyst at 553 K.

decomposition of DME, and favors the selective oxidation of DME to HCHO.

Thus, it can be seen that the oxidation of DME involves several products, such as HCHO, CO, CO_2, CH_3OH, CH_3OCOH and CH_4. Formaldehyde is the main primary product while CO and CH_3OH are the dominant by-products. Methanol is formed by intra-transfer of hydrogen between two CH_3O* species. CO can be produced directly by CH_3* oxidation or CH_3O* decomposition. CO can also be produced indirectly by secondary reactions of HCHO.

3.4 *Apparent activation energies and pre-exponential factors*

The activation energies and pre-exponential factors for the oxidation of DME were calculated according to the Arrhenius plots over the VO_x and MoO_x catalysts. The results are summarized in tables 2 and 3, respectively.

The apparent activation energy for the conversion of DME is 122 kJ/mol and the pre-exponential factor is 0.94×10^6 on the VO_x/Al_2O_3 catalysts. Although the activation energy for the formation of HCHO is slightly higher than that for the formation of CH_3OH, the pre-exponential factor for the formation of HCHO is nearly two orders of magnitude higher than that of CH_3OH. So the yield of HCHO is much higher than that of CH_3OH. In spite that the activation energy for CO formation is the highest, the highest pre-exponential factor for the formation of CO makes it the main by-product. The selectivity to CO_2 is always low owing to the much smaller pre-exponential factor of CO_2 formation.

Table 2
Kinetic parameters over VO_x/Al_2O_3 catalyst

	DME/O_2 = 1.48		DME/O_2 = 2.66		DME/O_2 = 5.03		Average	
	E_a (kJ/mol)	A (mol/gcat·s)	E_a (kJ/mol)	A (mol/gcat·s)	E_a (kJ/mol)	A (mol/gcat·s)	E_a (kJ/mol)	A (mol/gcat·s)
DME	118.9	4.34×10^5	123.8	1.37×10^6	122.7	1.02×10^6	121.8	0.94×10^6
HCHO	111.8	5.99×10^4	116.4	1.82×10^5	121.1	4.47×10^5	116.4	2.30×10^5
CO	150.2	1.00×10^8	155.4	3.19×10^8	145.2	3.33×10^7	150.3	1.51×10^8
CO_2	82.8	5.31	80.9	3.63			81.9	4.47
CH_3OH	106.1	1.19×10^3	114.7	1.35×10^3	111.7	8.27×10^3	110.8	3.60×10^3

Table 3
Kinetic parameters over MoO_x/Al_2O_3 catalyst

	DME/O_2 = 1.54		DME/O_2 = 2.76		DME/O_2 = 4.83		Average	
	E_a (kJ/mol)	A (mol/gcat·s)	E_a (kJ/mol)	A (mol/gcat·s)	E_a (kJ/mol)	A(mol/gcat·s)	E_a (kJ/mol)	A (mol/gcat·s)
DME	128.5	2.17×10^6	119.5	3.12×10^5	128.3	1.89×10^6	125.4	1.46×10^6
HCHO	121.6	3.66×10^5	117.3	1.44×10^5	125.2	7.37×10^5	121.4	4.16×10^5
CO	165.0	1.02×10^9	141.8	6.72×10^6	158.0	1.61×10^8	154.9	3.94×10^8
CH_3OH	102.8	4.03×10^2	100.4	2.90×10^2	118.1	7.33×10^3	107.1	2.67×10^3

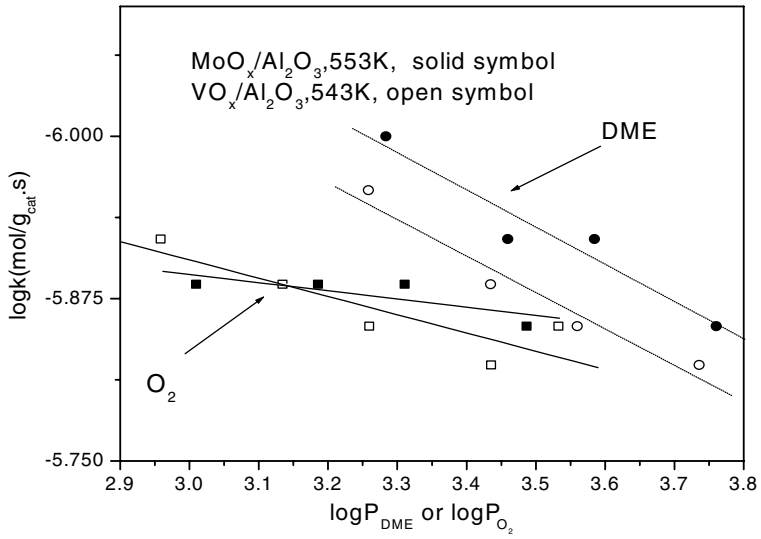

Figure 7. Reaction orders with respect to DME and O_2.

The activation energies and pre-exponential factors for DME conversion and product formation on the MoO_x/Al_2O_3 catalyst were also calculated. The observed kinetic behaviors on the MoO_x $/Al_2O_3$ catalyst are very similar to that on the VO_x $/Al_2O_3$ catalyst.

3.5. *Reaction orders*

The reaction result for the determination of the reaction orders with respect to DME and O_2 is listed in figure 7. The reaction rates did not change markedly with the variation in either the oxygen concentration or the DME concentration. Therefore, the reaction was pseudo-zero order with respect to the DME and the O_2 partial pressures employed. Increase of the gas phase concentration has little effect on the reaction rate.

This also means that DME can be initially decomposed easily into adsorbed CH_3 and CH_3O species on the MoO_x and VO_x catalyst surfaces [15]. Selective oxidation of DME is controlled by reactions of the saturated intermediates adsorbed. The zero-order dependence of O_2 indicates that the transformation of oxygen molecule into lattice oxygen, and the rapture of O species by dissociated CH_3* to form CH_3O* could not be the rate-limiting step. The reaction rate is most likely to be limited by the C–H bond activation of the adsorbed CH_3O* intermediate via a redox mechanism by using the lattice oxygen atoms as depicted following.

$$CH_3O\text{–s} + O\text{–s} \rightarrow HCHO\text{–s} + HO\text{–s}$$

$$2HO\text{–s} \rightarrow H_2O\text{–s} + O\text{–s}$$

4. Conclusions

Kinetics of DME oxidation has been investigated over Al_2O_3-supported VO_x and MoO_x catalyst near their monolayer capacity loadings. The effects of contact time on DME conversion and HCHO selectivity indicates that the reaction only takes place on the surface of the catalyst, and HCHO is the main primary product. The apparent activation energies for the conversion of DME were found to be 122 kJ/mol over the VO_x/Al_2O_3, and 125 kJ/mol over the MoO_x/Al_2O_3, respectively. The reaction is pseudo-zero order with respect to both DME and O_2 under the reaction conditions employed, suggesting that the most likely rate-determining step is the oxy-dehydrogenation of the CH_3O* species.

References

[1] J.L. Li, X.G. Zhang and T. Inui, Appl. Catal. A 147 (1996) 23.
[2] Haichao Liu and Enrique Iglesia, J. Catal. 208 (2002) 1.
[3] Guangyu Cai *et al.*, Appl. Catal. A 125 (1995) 29.
[4] F. Ouyang and S. Yao, J. Phys. Chem. B 104 (2000) 11253.
[5] L. Lefferts, J.G. van Ommen and J.R.H. Ross, Appl. Catal. 23 (1986) 385.
[6] J.M. Tatibouet, Appl. Catal. A 148 (1997) 213.
[7] Haichao Liu, Patricia Cheung and Enrique Iglesia, J. Catal. 217 (2003) 222.
[8] Xiumin Huang, Yide Xu and Wenjie Shen, Chin. J. Catal. 25 (4) (2004) 267–271.
[9] Haichao Liu, Patricia Cheung and Enrique Iglesia J. Phys. Chem. B, 107 (2003) 4118.
[10] Haichao Liu, Patricia Cheung and Enrique Iglesia, Phys. Chem. Chem. Phys. 5 (2003) 3795.
[11] Zhengping Li, Lian Gao and Shan Zheng, Appl. Catal. A. Gen. 236 (2002) 163–171.
[12] P. Wehrer *et al.*, Appl. Catal. A. Gen. 238 (2003) 69–84.
[13] Moon Young Shin, Chang Mo Nam, Dae Won Park and Jong Shil Chung, Appl. Catal. A. Gen. 211 (2001) 213–225.
[14] A. Pantazidis, A. Burrows, C.J. Kiely and C. Mirodatos, J. Catal. 177 (1998) 325–334.
[15] Shizhong Wang, Tatsumi Ishihara and Yusaku Takita, Appl. Catal. A 228 (2002) 167.